

# BEAM CHARACTERISTICS MEASUREMENT OF ITC-RF GUN FOR t-ACTS PROJECT\*

N.Y. Huang<sup>#,A,B)</sup>, H. Hama<sup>A)</sup>, S. Kashiwagi<sup>A)</sup>, F. Hinode<sup>A)</sup>, K. Takahashi<sup>A)</sup>, I. Nagasawa<sup>A)</sup>,  
T. Muto<sup>A)</sup>, K. Nanbu<sup>A)</sup>, Y. Shibasaki<sup>A)</sup>, M. Kawai<sup>A)</sup>,

A) Electron Light Science Centre, Tohoku University  
Sendai, Miyagi, 982-0826, Japan

B) Institute of Photonics Technologies, National Tsing Hua University  
101, section 2, Kuan-Fu Road, Hsinchu, 300, Taiwan

## Abstract

An energy spectrometer for the measurement of beam characteristics from an independently tuneable cells (ITC) thermionic RF gun which is developed for the test accelerator system for high intensity THz radiation source (t-ACTS) has been installed. The energy spectrometer is composed of a 45 degree bending magnet, a 0.5 mm width slit and the Faraday cup. Varying the input RF field strength and its phase separately, the beam properties produced from the ITC-RF gun can be manipulated. Since a linearly momentum chirped beam in the longitudinal phase space may be suitable for bunch compression, the energy spectrum of the beam extracted from the ITC-RF gun has to be well investigated. We report the preliminary experimental result and its analysis by comparing with the numerical simulation result.

## INTRODUCTION

In the t-ACTS project, the THz coherent synchrotron radiation (CSR) from a long period undulator will be provided as a narrow band THz source, and a dedicated isochronous ring will be worked as a wide band CSR source [1]. In order to achieve sufficiently large form factor for production of CSR in the THz frequency region, the bunch length less than 30  $\mu\text{m}$  (100 fs) is required. Hence, a stable production of short electron pulses is the key issue in this project. We have anticipated that the pulse train of very short bunches will be produced by means of velocity bunching in a traveling-wave accelerating structure [2].

The t-ACTS injector consists of the ITC thermionic RF gun equipped with a single crystal LaB<sub>6</sub> cathode, an alpha magnet and a 3 m-long accelerating structure. A 50 MW RF power is distributed to two cells of the ITC-RF gun and the accelerating structure. The RF phase differences among two cells and the accelerating structure are tuneable by phase shifters. Using RF attenuators, input powers are separately adjustable [3]. In order to compress the electron bunch by velocity bunching scheme, actual electron distribution in the longitudinal phase space is significant for choosing a proper initial RF phase in the accelerating structure. Therefore, we have installed an energy spectrometer to investigate the energy distribution of the beam from the ITC RF gun. Here, the experimental

result under the nominal operating condition in which the RF phase of the 2nd cell is ( $\phi_2$ )  $\pi+0$  degree with respect to that of the 1st cell ( $\phi_1$ ), the electric field on the cathode surface in the 1st cell ( $E_1$ ) and at the center of the 2nd cell ( $E_2$ ) are 25 MV/m and 70 MV/m, respectively, and the emission current density of the cathode is 50 A/cm<sup>2</sup> is reported.

As known well, thermionic RF gun provides a beam of which electrons are populated more densely at the head of the microbunch, and then the space charge effect may be serious especially at the top portion of bunch. From a beam tracking simulation by GPT [4], the particle distribution in the longitudinal phase space is much more different if space charge effect is included in the calculation. For example a derived momentum spread for the top 30 pC bunch reaches  $\sim 1.5\%$  that is about two times larger than the case of without space charge effect. In order to observe the detail at the top portion of particle distribution, an energy resolution less than 0.15 % is required for the spectrometer system.

## EXPERIMENTAL SETUP

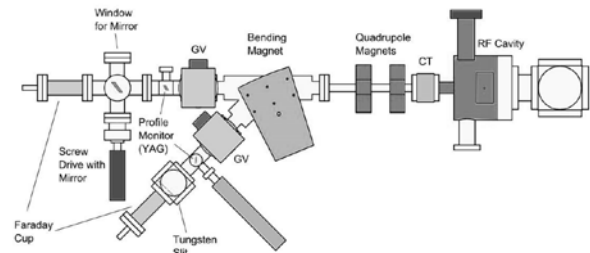


Figure 1: Experimental apparatus of the spectrometer.

The measurement setup is shown as fig. 1. There is a current transformer (CT) located at the gun exit to measure the total generated beam current. The 45 degree bending magnet downstream bends the beam into a beamline for the measurement of energy spectrum. There is a 0.5 mm width slit located on the central orbit at the downstream of the bending magnet. The faraday cup (FC) is at the end of this beamline to measure the charge of the transmitted electrons passing through the slit. The bending magnet is initially designed for the purpose of a 10 degree inverted bend in the isochronous ring. Therefore, there is a rotation angle of 17.5 degree at each pole face. This rotation angle at the pole face helps to

\*Work supported by Grant-in-Aid for Scientific Research (S), the Ministry of Education, Science, Technology, Sports and Culture, Japan, contract No. 20226003.

<sup>#</sup>nyhuang@ins.tohoku.ac.jp

focus the beam in the vertical direction. Betatron motion dependent beam size can be controlled by two quadrupoles located at the upstream of the bending magnet.

The nominal momentum of the electrons that is travelling on the central orbit is selected by changing the field strength of the bending magnet. The slit with a finite width enforces a certain amount of electrons transmit through it. In order to calibrate the magnetic field in the bending magnet, another identical bending magnet is serially connected to the power supply together with the spectrometer magnet. The identical one located outside the shielded experimental room is used for the measurement of magnetic field by employing a Hall probe. Because both magnets follow the same hysteresis process, we can measure the magnetic field and thus the nominal beam momentum simultaneously. Although the effective length of the fringe field of the bending magnet was expected by a 3-D field calculation, the accurate one has not been well defined yet. Accordingly the absolute value of the momentum at certain field strength has to be calibrated later.

## ESTIMATION OF MOMENTUM RESOLUTION

The beam should have finite beam size due to a transverse beam emittance. From the simulations, we have known that the momentum-sliced emittance in one micropulse is not constant and the Twiss parameters as well. Momentum resolution of the slit for the transmitted electrons is expressed by the convolution between the slit width (momentum aperture) and the betatron beam size as

$$\delta_p = \frac{\sigma_p}{P_c} = \frac{1}{\eta} \sqrt{\left(\frac{W}{2\sqrt{3}}\right)^2 + (\sigma_\beta)^2}, \quad (1)$$

where  $\eta$  is the dispersion function at the position of slit center,  $W$  is the full slit width,  $\sigma_\beta = \sqrt{\varepsilon\beta}$  is the betatron dependence beam size,  $\sigma_p$  is the standard deviation of momentum,  $P_c$  is the central momentum of electrons. The dispersion function is theoretically evaluated from the experimental configuration of the spectrometer which is 0.302 m at the position of the slit.

The ideal momentum resolution (absence of the beam

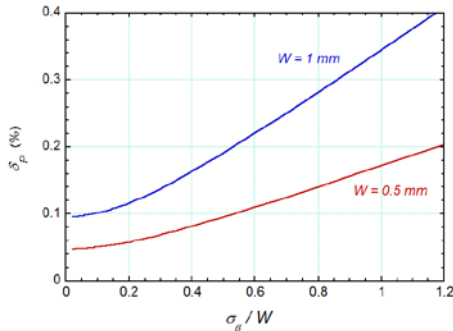


Figure 2: Estimated energy resolution using eq. (1).

emittance) is 0.048 % and 0.095 % for the full slit width of 0.5 mm and 1.0 mm, respectively. It is apparent from eq. (1) that the practical momentum resolution gets reduced as increasing of the betatron beam size. Figure 2 shows the estimated momentum resolution for two different widths of the slit.

As mentioned previously, the momentum resolution of 0.15 % is at least required to resolve the energy spectrum in the top portion of particles. Therefore, we have chosen the slit width of 0.5 mm that is able to offer the momentum resolution of 0.17 % when the transverse beam size is the same as the slit width. The estimated momentum resolution by using eq. (1) agrees well with the result deduced from tracking simulations by GPT. In addition, it was turned out that the horizontal beam size for which the beam is transported without quadrupoles is mostly less than 0.5 mm at the slit position, which results from the extra focusing effect of the fringe field in the bending magnet fortunately. We have also examined the momentum resolution can be improved to  $\sim 0.06$  % by employing proper quadrupole strengths.

## MEASUREMENT RESULTS AND DISCUSSION

### Calibration of RF phase and current density

In order to know the RF phase and the current density of the cathode, we have measured the extracted total beam current at the gun exit for different RF phases. The result is shown in fig. 3.

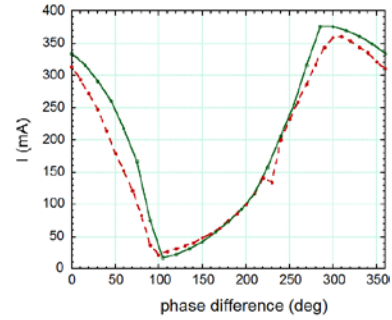


Figure 3: Total beam current as a function of RF phase difference between two cells. The red line is the experimental result when the heater current was set to be 9.95 A. The green line indicates the GPT simulation result by adapting phase differences to fit the experimental data.

Comparing with the simulation results, the operated RF phase was calibrated and the cathode current density had been well presumed. The emission current density of the cathode shall be  $\sim 50$  A/cm<sup>2</sup> when the heater current is 9.95 A.

### Preliminary experimental results

We have measured the signal from the CT and the FC under the nominal operating condition. Figure 4 shows a measured beam current for one macropulse by the CT.

The signal arises around 0.9  $\mu\text{s}$  and the pulse duration is about 2  $\mu\text{s}$ . The generated beam current achieves  $\sim 310$  mA after the RF filling time ( $t \sim 1.5$   $\mu\text{s}$ ) and it gradually increased because the cathode is additionally heated by back-streaming electrons, which is well-known as the back-bombardment effect.

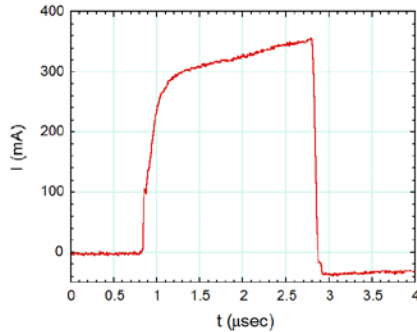


Figure 4: Measured beam current for a macropulse.

A two dimensional spectrum of the transmitted beam current passing through the slit measured from the FC is shown in fig. 5, where the beam momentum is selected by the corresponding magnetic field. At the beginning of this signal, it can be seen that the current and energy is increasing during the RF power is built up inside the cavity. After the RF filling time, a non-flat waveform is observed. The beam current is increased due to the back-bombardment effect. However the tail part of signal shows that the beam energy is slightly decreased due to the beam loading.

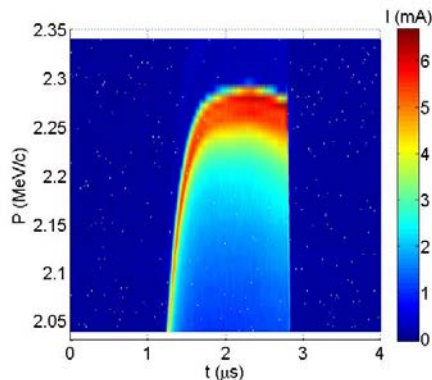


Figure 5: Beam current measured by the FC for different beam momentum. The vertical axis is transformed from the magnetic field measured in the pilot magnet.

### Discussion

For the experimental data of the nominal operating condition (the green line) as shown in fig. 6, the sharp forward peak is not observed as the expectation (the blue line). However when the RF power fed into the cathode cell is increased, the forward peak appeared (the red line). Although the measured beam current for the nominal operating condition seems to be much smaller than the simulation result, another experimental data looks better and closer. It implies that the actual coupled RF power into both cells may be smaller than we expected. On the

other hand, we can see a disagreement in momentum between the experimental and the simulation result. In addition to further momentum calibration of the system, we have to calibrate the RF power precisely.

At a glance, the momentum resolution of this measurement may be good as predicted. However the width of the forward peak is a bit wider than the simulation. At present we have not investigated yet if some instability was happened for the nominal operating condition. Since the stability of the ITC-RF gun has not yet confirmed, energy shift during measurement is not completely denied.

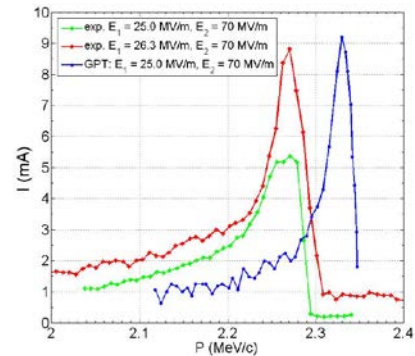


Figure 6: Measured energy spectra of the extracted beam for two different RF field strengths (the green and red lines). The simulated spectrum for the nominal operating condition is also shown (the blue line). The experimental data were measured at  $t = 2.0$   $\mu\text{s}$ .

## SUMMARY AND PROSPECT

We have installed an energy spectrometer to examine performance of the ITC-RF gun. The expected energy resolution of the spectrometer system is  $\sim 0.15\%$  without the assistance of quadrupole focusing. We clearly observed specific characteristics of themionic RF gun such as the back-bombardment and the beam loading effect. Though the experimental results suggest that further precise calibration for the system is highly desired, the spectrometer provides a good energy resolution is an excellent opportunity for us to understand the actual beam performance.

## ACKNOWLEDGEMENT

One of the authors (N.Y. H.) would like to thank the support of National Science Council, Taiwan (contract No. 101-2917-I-007-003) for this study in Electron Light Science Centre, Tohoku University.

## REFERENCES

- [1] H. Hama et al., in Proceedings of IPAC'11, San Sebastian, Spain, (2011), p. 2990.
- [2] N.Y. Huang et al., submitted to elsewhere.
- [3] S. Kashiwagi et al., in Proceedings of IPAC'11, San Sebastian, Spain, (2011), p. 2993.
- [4] GPT (general particle tracer), Pulse Physics, <http://www.pulsar.nl/gpt/index.html>.